Universidad Zaragoza
1542

# Trabajo Fin de Máster

## Título del trabajo: Terapia fototérmica mediante un fotosensibilizador intracelular: La Croconaina

## English tittle: Photothermal therapy using an intracellular photosensitizer: Croconaine dye


Autor/es

Clara Font Bernet

Director/es

Manuel Arruebo Gordo
Teresa Alejo Cuesta



MÁSTER EN INGENIERÍA BIOMÉDICA

ESCUELA DE INGENIERÍA Y ARQUITECTURA
2018

TRABAJOS DE FIN DE GRADO / FIN DE MÁSTER

Escuela de Ingeniería y Arquitectura Universidad Zaragoza

# DECLARACIÓN DE AUTORÍA Y ORIGINALIDAD

(Este documento debe acompañar al Trabajo Fin de Grado (TFG)/Trabajo Fin de Máster (TFM) cuando sea depositado para su evaluación).

D./Dª. CLARA FONT BERNET,

con nº de DNI 17777 en aplicación de lo dispuesto en el art. 14 (Derechos de autor) del Acuerdo de 11 de septiembre de 2014, del Consejo de Gobierno, por el que se aprueba el Reglamento de los TFG y TFM de la Universidad de Zaragoza,

Declaro que el presente Trabajo de Fin de (Grado/Máster) Máster, (Título del Trabajo) Photothermal therapy using an intracellular photosensitizer: Croconaine Dye (Terapia fototérmica mediante un fotosensibilizador intracelular: La Croconaina),

es de mi autoría y es original, no habiéndose utilizado fuente sin ser citada debidamente.

Zaragoza, 30 de Enero del 2018

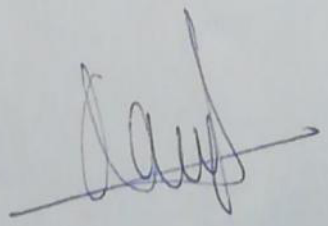

Fdo: CLARA FONT BERNET

# TERAPIA FOTOTÉRMICA MEDIANTE UN FOTOSENSIBILIZADOR INTRACELULAR: LA CROCONAINA

## RESUMEN

El mundo de la nanomedicina aplicada en el tratamiento de cáncer está creciendo muy rápidamente. De hecho, a lo largo de las últimas décadas se han diseñado muchas nanoterapias como alternativa o mejora de las terapias ya existentes contra el cáncer y contra las enfermedades infecciosas principalmente. Una de ellas, la terapia fototérmica, tiene como finalidad el aprovechar el calor emitido por algunos agentes fototérmicos al absorber luz en el infrarrojo cercano (NIR), para poder así destruir células cancerígenas por ablación térmica. Por otro lado, la croconaina es una molécula ya estudiada como agente fotosensibilizante por su dualidad estructural y de absorbancia frente a cambios de pH, presentando una importante absorción en 800 nm cuando se encuentra en medio ácido (pH 5). Esta característica resulta interesante para una terapia fototérmica más segura y efectiva que solo permite la inactivación de las células cuando se encuentra en su interior (ya que algunos compartimentos intracelulares, endosomas, son ácidos) pues el medio extracelular es ligeramente alcalino.

En este trabajo se presenta la compleja síntesis de la croconaina incluida en un macrociclo para evitar su posterior agregación y posible *quenching* de absorbancia. Asimismo, se muestran nuevas encapsulaciones de croconaina que se han llevado a cabo tanto en nanopartículas poliméricas, mediante nanoprecipitación o doble emulsión, como en niosomas. Estas innovadoras encapsulaciones exhiben beneficios frente a los liposomas ya utilizados para encapsular dicha molécula, pues tienen una mayor estabilidad y reducidos costes. También se resalta la dificultad de lograr el comportamiento dual en medio ácido y alcalino de las nanopartículas cargadas de croconaina, debido a la baja difusión del medio en la nanopartícula, impidiendo su cambio de estructura, o bien de la posible baja concentración de molécula encapsulada dentro de las nanopartículas. Todas las síntesis químicas se han caracterizado mediante resonancia magnética nuclear (RMN), y todas las síntesis de nanopartículas se han caracterizado mediante técnicas de visualización ya sea mediante microscopía electrónica de barrido (SEM) o mediante microscopía electrónica de transmisión (TEM). Por otro lado, el comportamiento fototérmico de la croconaina y las nanopartículas se ha evaluado mediante ensayo espectroscópico de absorción UV/VIS y mediante la monitorización de la temperatura al irradiar las muestras con un láser de 808 nm.

Finalmente, se ha comprobado la baja citotoxicidad de la molécula en cultivos celulares de monocitos, y su imposible aplicación, a las dosis estudiadas y con las irradiancias usadas, como agente de terapia fototérmica para la ablación de *Estafilococos Aureus* en infecciones a causa de la alta resistencia térmica de dicha cepa bacteriana.

# PHOTOTHERMAL THERAPY USING AN INTRACELLULAR PHOTOSENSITIZER: CROCONAINE DYE

## ABSTRACT

Nanomedicine is growing quickly, especially for cancer treatment. In fact, many nanotherapies against cancer have been developed over the past decades as an alternative or an improvement of the exiting cancer and antimicrobial therapies. Among them, photothermal therapy's purpose is to use the heat emitted from photothermal agents when they absorb near-infrared (NIR) light, to damage and destroy tumoral cells by heat ablation. On the other hand, croconaine dye is a widely used photosensitizer due to its structural and absorbance duality depending on pH variations, presenting a remarkable absorbance peak at 800 nm when found in an acidic medium (pH 5) and remaining un-activated under physiological conditions. This feature turns out to be interesting to ensure a safer and more efficient photothermal therapy, which would only allow cell inactivation when located inside the cell because intracellular compartments (endosomes) are acidic.

In this study, a complex synthesis of the croconaine dye trapped into a macrocycle to avoid its self-aggregation and possible absorbance quenching, is presented. Moreover, new croconaine encapsulations are shown, with polymeric nanoparticles, by nanoprecipitation or double emulsion methods, and within niosomes. These novel encapsulations exhibit some advantages compared to the already used liposomes to encapsulate this molecule, since they are known for their high stability and low costs. The struggling of achieving the croconaine loaded nanoparticles dual behavior in an acidic and alkaline medium is also highlighted, which is related to the reduced medium diffusion into the nanoparticle, preventing its structure shift, or the possible low croconaine concentration encapsulated within the nanoparticles. All the chemical syntheses have been characterized by Nuclear Magnetic Resonance (NMR), and all the nanoparticle syntheses have been characterized by Scanning Electron Microscopy (SEM) or Transmission Electron Microscopy (TEM). On the other hand, the photothermal behavior of both free croconaine and croconaine loaded nanoparticles have been evaluated by UV/VIS absorption spectroscopy and by temperature monitoring when irradiated with an 808mn laser.

Finally, a reduced cytotoxicity of the molecule has been proved with monocytes cell cultures at the doses tested, just as their negligible photothermal effect at the doses and irradiances tested in the ablation of *Staphylococcus Aureus* in infections due to the high thermal resistance of this bacterial strain.

# TABLE OF CONTENTS

# Chapter 01

## 1. INTRODUCTION

Nanotechnology term was first described by Tokyo Science University Professor Norio Taniguchi in 1974, who held that "Nano-technology mainly consists of the processing of, separation, consolidation, and deformation of materials by one atom or by one molecule" [1]. We are talking about the nanoscale where the ratio between a nanoparticle and a soccer ball remains equal as this same ball and the earth. Nanotechnology mixes many techniques in order to manipulate matter on an atomic and molecular level. This is why it is called an interdisciplinary field that uses physics, biology, chemistry and computing, among others [2]. Actually, it is widely used in the industry, including the food industry, cosmetics, electronic or medical disciplines.

Concerning this last discipline, nanomedicine is one of the most promising branches for the advance of the current medicine, allowing localized treatments at a cellular and molecular level. It can also be applied in diagnostics, disease or treatment monitorization, pain relief or drug delivery, among many other applications. Nanomedicine interest resides in the possibility to engineer nanoparticles (NPs) as desired, so the *in vivo* behaviour will be optimal [3][4]. Some of the NPs features that can be modified are the shape, size or surface functionalization emulating, for example, the existing viruses, such as HIV virus (spherical shaped), or bacteria [3]. In fact, they all stand in a nanoscaled sized, remaining smaller than a white blood cell and larger than a glucose molecule [5] (Figure 1).

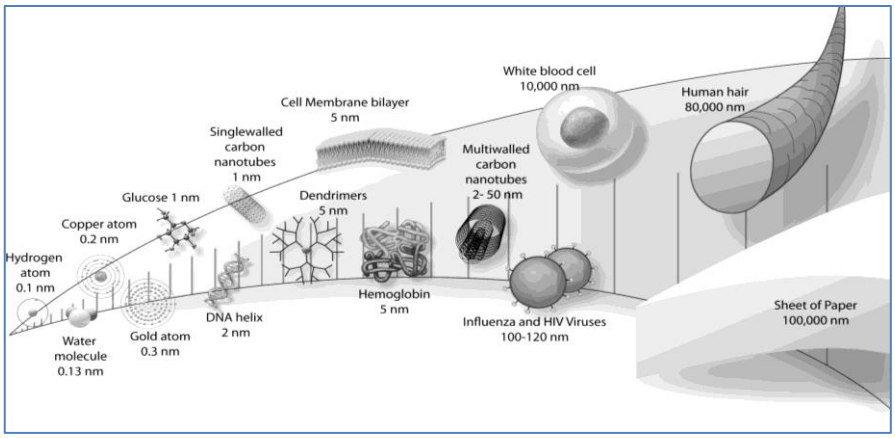


*Figure 1. Nanosized biomaterials compared in a bionanoscale. (R. Yokel et al. 2011)* [5]

Considering the nanoparticle sizes together with the immature tumor vasculature, the idea of applying nanomedicine against cancer came up in the 80's and grew swiftly. A fast development of new blood vessels in tumors, also known as tumor angiogenesis, in order to meet the high oxygen and nutrient demand, results as an irregular and leaky structure that allows particles smaller than 0.1-3 µm to cross through (Figure 2). On the other hand, a reduced lymphatic drainage favors the accumulation of these nanoparticles in the tumor tissue. This passive phenomenon is known as Enhanced Permeability and Retention (EPR) effect, and it varies within patients and solid tumor types [4][6][7][8][9]. Even if the pores of this incomplete endothelial lining are about 0.1-3 µm (diameter), a too large nanoparticle will be quickly identified and trapped by the reticuloendothelial system. Therefore, an appropriate maximum nanoparticle size oscillates between 200-400 nm for this kind of nanotherapies. Nevertheless, if the nanoparticles are too small (<3-6 nm), they will rapidly be excreted by the kidneys [6][7][10].

The EPR effect does not affect normal tissue because of the endothelial vessel's cells tightness, avoiding unnecessary harm to healthy cells by the nanotherapeutic use [11].

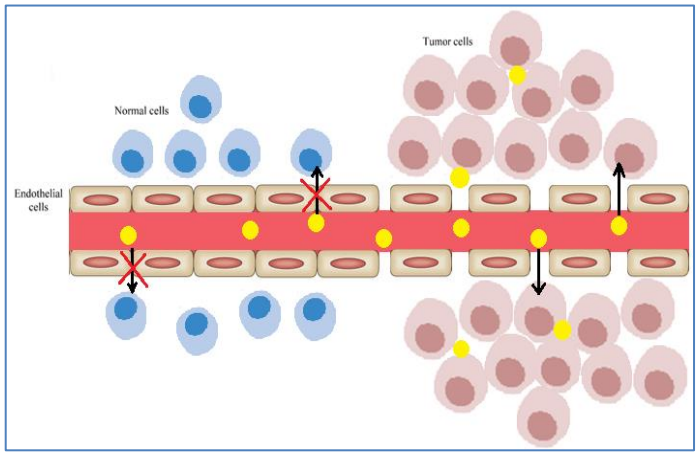


*Figure 2. Cartoon of a regular tight capillary (on the left) versus a tumor leaky capillary (on the right). The yellow nanoparticles can get through the pores and reach the tumor cells but not the healthy ones.*

Nowadays, there are many lines of research concerning nanotherapies applied to cancer treatment. Several nanoparticles have already been approved by the Food and Drug Administration (FDA), such as liposomes (for example Doxil®) or some albumin-based micelles as drug deliverers. However, many other therapies are under investigation in a clinical level. Some of them are gene or RNA interference (RNAi) therapy, photodynamic therapy or photothermal therapy, among others [4]. Regarding this last one, photothermal therapy (PTT) basis consists on a photosensitizer capable of absorbing light at a specific wavelength and release vibrational energy producing a heat increase. When this heat rises up above 43ºC, the denaturation of proteins is induced and therefore the apoptosis of normal and tumoral cells occurs [6][12]. Along all the thermal therapies, PTT is known as a minimal invasiveness technique with a high specificity and efficacy and low toxicity to healthy tissues, that it can be

combined with existing cancer therapies [13][14]. These advantages are achieved by using laser irradiation at near-infrared (NIR) frequencies (700 - 1100 nm). The NIR light is able to penetrate deeply into the tissues without harming healthy cells since neither water, blood cells or biological tissues can strongly absorb these wavelengths [11][12][14]. Regarding to the NIR light absorbing agents used in PTT, they should be non-toxic and biocompatible such as inorganic ones (gold nanostructures, carbon materials or copper sulfide nanoparticles, etc.) or organic ones (indocyanine green (ICG), IR780, IR-808, etc.) [6][11][13][14]. These last small molecular organic dyes show relevant advantages, including a good reproducibility in their effects, a very well defined molecular structures, strong absorption at NIR wavelengths and enhanced biodegradability [13][14].

However, even if ICG has been widely used in PTT, it shows a poor photostability, high fluorescence quenching and cannot be chemically modulated [15], hence recent studies have presented a new chromophore, the croconaine, that has the ability to alter its structure depending on the local chemical environment [16]. It actually has a dual behavior depending on the environmental pH, switching its structure and its absorption profile from an alkaline form (absorption peak at 660 nm at a pH 7.4) to an acidic form (high absorption peak around 800 nm at pH 2) (Figure 3) [16]. Moreover, croconaine dyes have a strong resistance to photobleaching and good chemical and thermal stability and show a short-excited state lifetime. They also have very little fluorescence emission and reduced singlet oxygen generation; thus, no photodynamic therapy will interfere with its photothermal effect. Nevertheless, they are not soluble in water, which is a drawback for *in vivo* biomedical use [15][16][17].

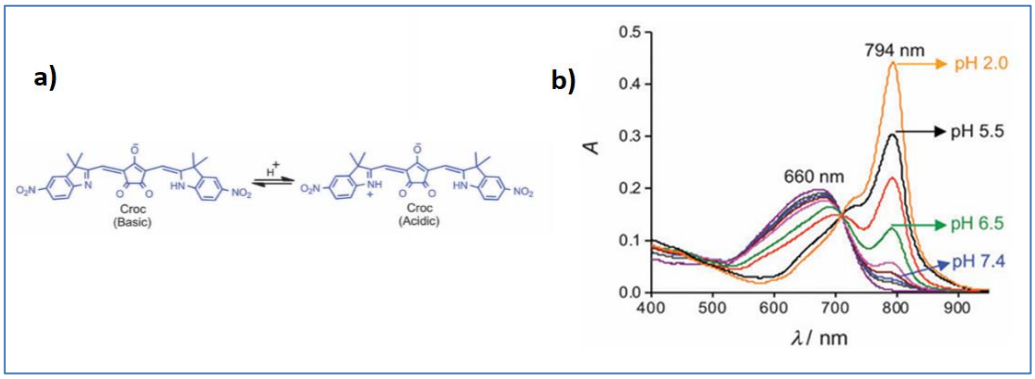


*Figure 3. a) Croconaine structure in both alkaline and acidic ph. b) UV/VIS absorption spectra of croconaine at different pH values. (S. Guha et al. 2016)* [16]

This structural shift determined by the pH of the medium can be very useful for a more controlled, effective and safe therapy. The extracellular pH, under physiological conditions, is about 7.3-7.4 (alkaline) [18], keeping the croconaine molecule on its alkaline structure. On the other hand, since the uptake of nanoparticles occurs mainly via endocytosis, more specifically the pinocytosis pathway (for particles smaller than 0.15 µm) [3], the pH inside the endosome would reach 5.5, meaning an acidic structure of the molecules and thus a high absorption around 800 nm will be found inside of endocytic vesicles [17]. This fact not only reinforce the hypothesis that this therapy will not cause any harm to neighboring healthy cells without the dye inside, but will also suggests a new hypothesis considering that cell-death will be more efficient when the molecules are located inside the cell [17][19].

As previously mentioned, the drawback of this molecule is its insolubility in water, thereby an encapsulation is needed to enhance the dye internalization and prolong its circulation time. The use of biodegradable polymeric nanoparticles for biomedical applications has increased over the past decade for their non-toxicity, their natural elimination by regular metabolic

pathways and their physical properties, such as hydrophilicity [20][21]. The use of Poly Lactic-co-Glycolic Acid (PLGA) nanoparticles has been studied for many research groups all over the world due to their favorable biodegradation and biocompatibility and wide possibilities for controlled drug delivery applications [21][22]. It actually is an FDA accepted copolymer in many devices made of Poly Lactic Acid (PLA) and Poly Glycolic Acid (PGA) [21][23]. Moreover, combining PLGA with Polyethylene Glycol (PEG), a higher hydrophilicity, stability and an enhanced imperceptibility for the immune system (by steric and hydrated repulsion) are reached increasing blood circulation time [21][23][24].

There are many PLGA nanoparticle synthesis mechanisms, such as simple emulsion, double emulsion, spray drying or nanoprecipitation among others [21][22][23][25]. Nanoprecipitation method is a very common technique due to its process simplicity, low cost and good reproducibility and controllable properties for the resulting NPs. Essentially, this process involves the polymer and the hydrophobic drug/dye dissolved in an organic solvent and an aqueous phase vigorously stirred where the organic one will be drop wise poured. When the polymer puts in contact with the water, it starts a nucleation process enclosing the hydrophobic medium inside and growing until a good stability is reached. The organic solvent diffuses out to the aqueous media and the polymer becomes insoluble. PLGA chains remain inside the nanoparticle and PEG chains are oriented to the water [22][23] (Figure 4a). On the other hand, double emulsion, also known as water-oil-water (w/o/w) emulsion method is suitable for encapsulating either hydrophobic or hydrophilic drugs. In this case, this method emulates the liposomes previously used for the croconaine dye encapsulation by S. Guha et al. [16]. Basically, a first water-oil emulsion is achieved by mixing the organic phase, where the polymer and the hydrophobic drug will be dissolved, with the aqueous phase. Next, a second emulsion is produced adding this first one into an aqueous solution. In this sort of process, a surfactant is needed to keep the structure together (Figure 4b) [21][25][26].

Likewise, another nanoparticle, structurally analogous to liposomes, has been studied in some research groups, the so-called niosome. These structures are made up of a bilayer of non-ionic surfactant (Spans or Tweens) instead of phospholipids (Figure 4c), which results in a more economical alternative with a higher chemical stability, due to their hard oxidation and potential hydrolysis while stored [27][28]. They can be unilamellar or multilamellar (Figure 4d), enclosing both hydrophobic or hydrophilic drugs [29]. Usually some membrane additives are used to improve the properties of the niosomes. For instance, one of the most used membrane additive is cholesterol which provides rigidity, stability, proper shape and enhanced entrapment efficiency [30]. It also often includes charge inducers to enhance their electrostatic stability, such as dihexadecyl phosphate (DCP) as anionic surfactant, increasing the surface charge density and avoiding their self-aggregation [28].

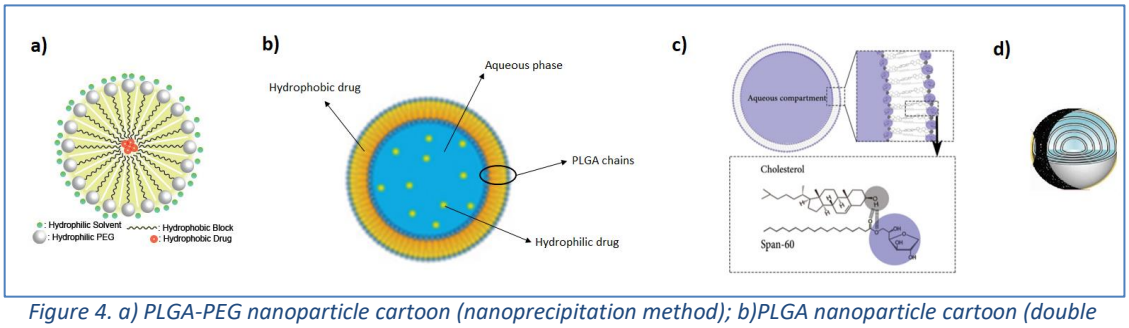


*Figure 4. a) PLGA-PEG nanoparticle cartoon (nanoprecipitation method); b)PLGA nanoparticle cartoon (double emulsion method); c) Unilamellar niosome cartoon (S. Moghassemi et al. 2014)* [31]*; d) Multilamellar niosome.*

However, none of these methods would be suitable unless the croconaine molecules were enclosed and trapped within a tetralactam macrocycle (Figure 5), avoiding their self-aggregation and thus their absorbance quenching in the reduced nanoparticle's inner space [16].

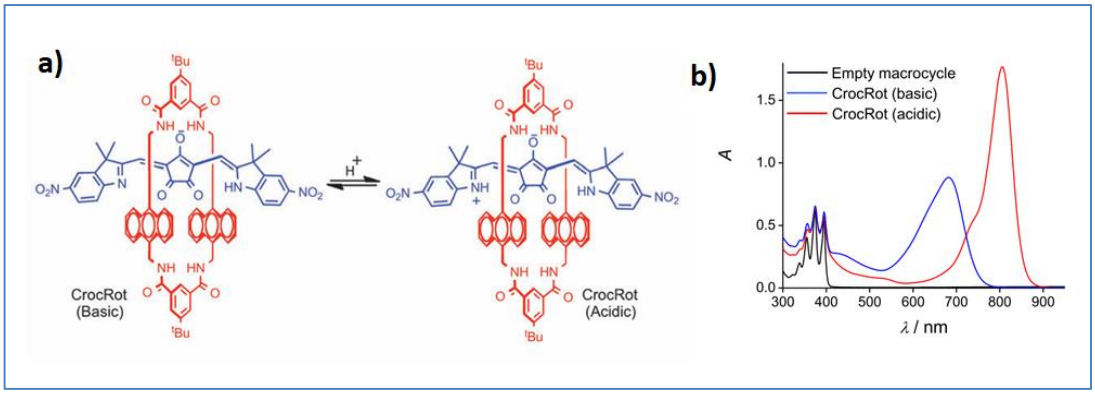


*Figure 5. a) Croconaine-macrocycle structure in both alkaline and acidic ph. b) UV/VIS absorption spectra of croconaine-macrocycle at acidic and alkaline pH, and empty macrocycle. (S. Guha et al. 2016) [16]*

Finally, this molecule can also be used as a wound-infection treatment, to eradicate bacteria independently or combined with antibiotics. Several groups have already tested PTT to treat dental infections [32], or treating wounds infected by pathogenic bacteria as a solution of the antibiotic resistance development of some bacteria [33]. *Staphylococcus Aureus* is a widely studied bacteria and one of the most dangerous existing staphylococcus. Cutaneous infections can cause blisters, abscesses and redness and swelling of the infected area and they are highly contagious [34]. Therefore, the last approach suggests a high enough acidification of the medium once the *S. Aureus* colony has infected the wound, and this effect could be used to produce a quick elimination of the *S. Aureus* by PTT using croconaine if a high enough temperature were reached because the growth of bacteria reduces the pH of the medium [35].

# Chapter 02

## 2. OBJECTIVES

Herein, polymeric nanoparticles with intracellular photothermal capacity will be developed. The purpose of this work is to cause tumor cell death selectively, only and exclusively when nanoparticle internalization has taken place, avoiding cell death when they are in the extracellular environment (Figure 6). Since croconaine shows excellent absorption in the NIR region when found in an acidic environment, it is chosen as the absorbing agent to generate localized heating. Moreover, free croconaine will be tested as a wound infection solution, trying to eliminate bacteria through thermal ablation.

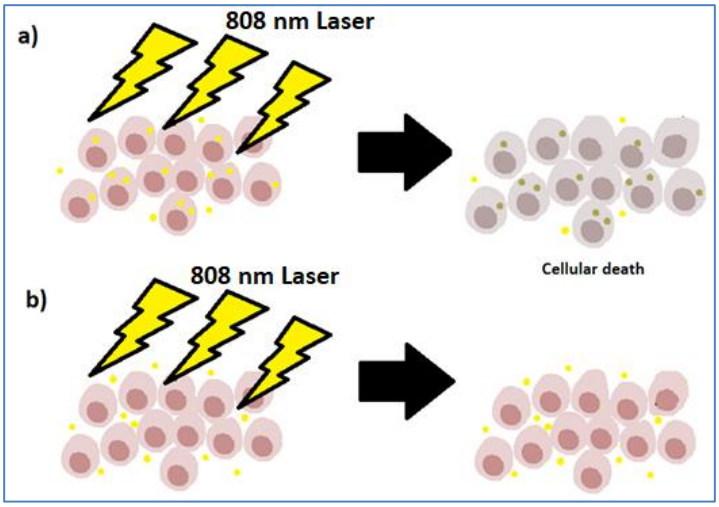


*Figure 6. Cartoon of the PTT using croconaine as a NIR absorbing agent. The nanoparticles with the croconaine are represented by yellow dots. a) The NPs internalized inside the endosomes of the cells, absorb the light at 800 nm and thus causing cellular death; b) no NPs are internalized by the cells, so none of the particles will absorb the NIR light and no cells will be affected.*

More specifically, to achieve these objectives:

- The croconaine molecule will be synthesized, characterized and trapped within a macrocycle.

- The final molecule will be encapsulated in PLGA-PEG nanoparticles using the nanoprecipitation method, in PLGA nanoparticles using double-emulsion method and within niosomes using dry film re-hydration method.

- The photothermal behavior of the final molecule and the croconaine loaded nanoparticles will be characterized.

- The final molecule and the nanoparticles will be tested *in vitro* to verify their cytotoxicity and their photothermal ability.

- The efficiency of the final molecule will be tested on an *in vitro* model of bacterial infection.

# Chapter 03

## 3. MATERIALS AND METHOD

### 3.1. CHEMICALS

2,3,3-Trimethylindolenine (98%), sodium nitrate ($NaNO_3$, 98%), sulfuric acid ($H_2SO_4$, 98%), sodium hydroxide (NaOH, ≥98%), ethyl acetate (EtOAc), magnesium sulfate ($MgSO_4$, ≥99.99%), croconic acid (98%), 1-butanol (anhydrous, 99.8%), toluene (anhydrous, 99.8%), ether (≥99.7%), anthracene, aqueous hydrobromic acid (HBr, 47%), glacial acetic acid (100%), 1,3,5-trioxane (≥99%), tetradecyltrimethylammonium bromide (TTA), ethanol (95%), hexamethylenetetramine (≥99%), chloroform ($CHCl_3$, 99.9%), chloroform ($CHCl_3$, anhydrous, ≥99%) hydrochloric acid (HCl, 37%), sodium carbonate ($Na_2CO_3$, ≥99%), 5-tert-butylisophthalic acid (98%), benzene (99.8%), dimethylformamide (DMF), thionyl chloride ($SOCl_2$, ≥99%), acetone ($C_3H_6O$, ≥99%), deuterated chloroform ($CDCl_3$, 99.96%), dihydrorhodamine 123 (DHR123, ≥95%), phosphate buffered saline (PBS), poly(ethylene glycol) methyl ether-block-poly(L-lactide-co-glycolide) (PLGA-PEG, PEG Mn 5,000, PLGA Mn 25,000, lactide:glycolide 50:50), poly(lactic-co-glycolic) (PLGA, RG504), sodium cholate (≥97%), poly(allylamine hydrochloride) (PAH, $M_W$ ~15,000 Da), hexadecyltrimethylammonium bromide (CTAB, 99%), cholesteryl 3β-N-(di-methyl-amino-ethyl)-carbamate hydrochloride (DC-Cholesterol) , sorbitan mono-oleate 20 (SPAN® 20), cholesterol, dihexadecyl phosphate (DCP), isopropyl alcohol (≥98%) and phosphotungstic acid (PTA) were purchased from Sigma-Aldrich. All of these chemicals were used as received without further purification. Human monocytes (THP-1) (*ATCC*), *Staphylococcus Aureus*, RPMI-1640 medium (*Gibco, TFS*), trypticase soy broth (TSB), tryptic soy agar (TSA) (*Condalab*), fetal bovine serum (FBS) (*TFS*), glutamine, non-essential amino acids (NEAA), HEPES, sodium pyruvate (*Biowest*), 2-mercaptoetanol (*Gibco, TFS*), penicillin-streptomycin-fungizone (PSA) (*Biowest*), CellQuanti-Blue reagent (*Abnova*), phorbol 12-myristate 13-acetate (PMA), acetic acid ($CH_3COOH$, ≥99.5%), dimethyl sulfoxide (DMSO, ≥99.7%) and gelatin solution 0.1% (*Sigma-Aldrich*).

## 3.2. ORGANIC SYNTHESIS

***Synthesis of Croconaine:***

The croconaine molecule (Figure 7) was synthesized following a procedure described by S. Guha et al. [16] (ANNEX I). Chemical structure of the final compound was confirmed by proton nuclear magnetic resonance spectroscopy ($^{1}$H-NMR), as shown in ANNEX II, Figure 37.

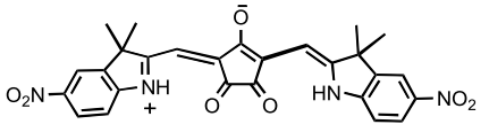


*Figure 7. Chemical structure of croconaine, S. Guha et al.* [16].

***Synthesis of Croconaine-macrocycle:***

Two separate compounds were needed for the croconaine encapsulation inside the macrocycle. 5-(tert-Butyl)isophthaloyl dichloride was obtained from the transformation of a 5-tert-butylisophthalic acid into an acyl chloride as described by A. Bugarin et al. [36] (ANNEX I). On the other side, 9,10-bis(aminomethyl)anthracene was synthetized in two steps. First, a 9,10-bis(bromomethyl)anthracene was obtained from a procedure reported by B. Alatava et al. [37] improving the purification process. In order to remove the remaining anthracene, the solid was filtered and washed with warm ethanol (60°C) three times, acquiring a 90% yield. Finally, the crude was reacted with hexamethylenetetramine getting 117 mg (50% yield) of 9,10-bis(aminomethyl)anthracene as reported by J. Gassensmith et al. [38] (ANNEX I). Chemical structure of each compound obtained was confirmed by nuclear magnetic resonance spectroscopy ($^{1}$H-NMR and $^{13}$C-NMR), as shown in ANNEX II, Figures 38 to 42.

The croconaine-macrocycle (Figure 8) was synthetized as described by S. Guha et al. [16], using a modification in the purification process. Two chromatographic columns were needed to purify the final product, a first one using a solution of chloroform and acetone (98% - 2%) as eluent, and a second one using chloroform (100%). The adequate concentration of solvents (acetone and chloroform), which separates the precursors by their polarity, was previously established using thin-layer chromatography (TLC). To ensure the product obtained was the croconaine trapped into the macrocycle, nuclear magnetic resonance spectroscopy (NMR) and two-dimensional nuclear magnetic resonance spectroscopy (COSY) were performed (ANEXO II, Figures 43 and 44). 18 mg of the product desired were finally as a result of a 10% yield.

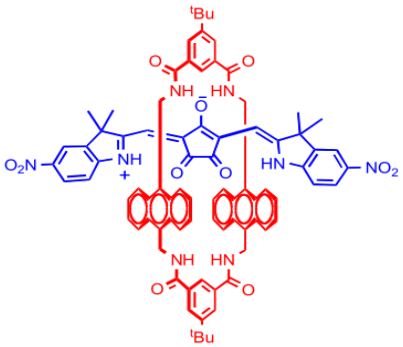


*Figure 8. Chemical structure of croconaine-macrocycle, S. Guha et al.* [16]

## 3.3. NANOPARTICLE SYNTHESIS

***Nanoprecipitation method:***

PLGA-PEG nanoparticles were carried out using a modification of the nanoprecipitation method reported by J. Cheng et al. [39]. Briefly, a solution of PLGA-PEG in acetone (5 mg/mL) was poured drop wise via a mechanical pump (2 mL/h) to a vigorous stirring water (1:1 volume) at room temperature. The organic solvent remaining was removed by evaporation while stirring for 2 h. The final mixture was washed with distilled water three times by centrifugation (6000 rpm, 10 min), and finally kept suspended in distilled water. For the encapsulation of croconaine, the molecules were solved in the organic solution (250 µg/mL).

***Double emulsion method:***

For the synthesis of PLGA nanoparticles using a double emulsion method (w/o/w), the procedure described by E. Luque-Michel et al. [26] was followed with some modifications. A first organic solution was prepared with 50 mg of PLGA and 1mL of ethyl acetate. A second aqueous solution was prepared with 50 µL of water and added into the organic solution. The mixture was sonicated for 15 s using an ultrasonic probe at 30% amplitude. The sodium cholate used as surfactant (2 mL, 1%) was then poured into the formed emulsion (w/o) and sonicated for 15 more seconds at 30% amplitude. This final double emulsion was added into 10 mL of sodium cholate (10%) and left under mechanical stirring for 3 h to allow solvent evaporation. A first wash was performed by centrifugation at 4500 rpm (10 min), and a second one at 7500 rpm (10 min). The final product was resuspended in distilled water. For the encapsulation of croconaine, the molecules were dissolved in the organic solution (3% molar ratio).

When other surfactants were used, as PAH, CTAB and DC-Cholesterol, the same molar ratio was used.

***Niosomes synthesis:***

Niosomes were prepared following a modification of the thin-film hydration procedure described by Paolino et al. [29]. Succinctly, 26 mg of SPAN® 20, 29 mg of cholesterol and 4.3 mg of DCP (47.5:47.5:5 molar ratio) were mixed together and dissolved in 200 µL of ethyl acetate in a 60ºC water bath for 5 min. The organic solvent was removed by evaporation under nitrogen flux for 3 h and then left overnight in a desiccator. After complete solvent evaporation, the film was resolubilized with 200 µL of isopropyl alcohol in a 60ºC water bath for 5 min and then mixed with 10 mL of Milli-Q water at 35ºC. The mixture was sonicated with an ultrasonic probe along ten cycles of 60 seconds each followed by 30 seconds pause (30% amplitude output). The remaining organic solvent was evaporated under mechanical stirring for 1 h. When the croconaine was encapsulated, a 3% molar ratio was mixed along the solid compounds in ethyl acetate.

When other surfactants were used, as PAH and CTAB instead of DCP, the same molar ratio was used.

***Characterization of nanoparticles***

The characterization of the nanoparticles size, polydispersity and morphology was carried out by Dynamic Light Scattering (DLS), Scanning Electron Microscopy (SEM) and Transmission Electron Microscopy (TEM).

TEM's sample preparation was performed using PTA (3 wt.%) as negative staining agent, to improve the contrast of the polymeric NPs. Samples were dropped in carbon coated copper grids. Then PTA was left 10 min in contact with the samples, washed with distilled water and dried at room temperature.

SEM's samples preparation was carried out on silicon wafers and using a gold-palladium (Au-Pd) coating to allow electronic observation.

***UV/VIS characterization***

Acidic and alkaline solutions were prepared depending on the sample. When free croconaine and free croconaine-macrocycle were tested, ethanol-HCl (pH 5) and ethanol-NaOH (pH 8) solutions were used having a concentration of 16 µM of the dye molecule. When empty and loaded nanoparticles were tested, $H_2O$-HCl (pH 5) and $H_2O$-PBS (pH 7.4) buffers were used, having 100 µL of the sample in 1 mL of buffer. Absorbance was measured from 200 nm to 1000 nm.

***Laser-Induced Heat Generation Studies:***

Croconaine and croconaine-macrocycle were dissolved in ethanol-HCl (pH 5) and ethanol-NaOH (pH 8) solutions at a 16 µM concentration. 1 mL of the solution was irradiated using an 808 nm-laser diode with the beam passing through it while stirring. The laser density power was set at 2 W/cm$^2$. The temperature was monitored by a thermocouple immersed into the solution, recording the temperature every 0.017 s.

***Reactive oxygen species (ROS) study***

The ROS liberation was evaluated following a modification of the procedure reported by B. Brawek et al. [40]. Dihydrorhodamine123 (DHR123) was used as the indicator of ROS presence [41][41][42]. A solution containing 6.6 µM DHR123 and 16 µM croconaine-macrocycle in an acidic medium (ethanol-HCl) was tested. The samples' fluorescence was quantified in a fluorescence spectrometer set at 480 nm for excitation, after 5 min and 10 min of laser irradiation (800 nm, 2 W/cm$^2$). Some controls were performed using a solution of DHR123 (6.6 µM) after 5 min stirring and after 5 min of irradiation, a solution of croconaine-macrocycle (16 µM) after 5 min stirring and after 5 min of irradiation, a solution of DHR123 (6.6 µM) and Croconaine-macrocycle (16 µM), after 5 min and 10 min stirring, and after 5 min warmed up in a water bath at 46ºC.

## 3.4. BIOLOGICAL STUDIES

***Cell assays:***

RPMI-1640 medium (500 mL) was supplemented with 50 mL of FBS (10% (v/v)), 5.5 mL of stable glutamine (2 mM), 5.8 mL of NEAA (1%), 5.8 mL of HEPES (10 mM), 5.8 mL of sodium pyruvate (1 mM), 0.58 mL of 2-mercaptoetanol (0.05 mM) and 5.5 mL of PSA (60 µg/ml penicillin, 100 µg/ml streptomycin and 0.25 µg/ml amphotericin B).

THP-1 monocytes were incubated in T75 flasks at 37ºC (5% $CO_2$) with RPMI 1640 medium (300.000 cell/mL). The medium was replaced every 48 h by centrifugation at 1500 rpm at room temperature for 5 min. The pellet was resuspended with fresh medium and 300.000 cell/mL were replaced in the flask. For the following experiments THP-1 cells were differentiated into macrophages, by seeding them in a 96-well culture dish (100 µL per well of a suspension of 700.000 cell/mL) previously prepared with gelatin solution (50 µL/well, 30 min), in presence of 10 µL of PMA (1:1000 µL). The plate was incubated for 72 h at 37ºC (5% $CO_2$).

Cytotoxic effects of free croconaine were evaluated by the Blue Cell Viability Assay Kit, following Abnova's protocol [43]. After differentiation of THP-1 monocytes into macrophages, the medium was removed, and the cells were washed twice with PBS. 100 µL of free croconaine at 75 µM (0.2% v/v DMSO), 37.5 µM, 18.75 µM, 9.38 µM, 4.69 µM, 2.34 µM of dissolved RPMI 1640 medium were added in every well. Two positive controls were prepared with 100 µL of RPMI 1640 and 100 µL of RPMI 1640 (0.2% v/v DMSO). A blank control was prepared with croconaine at 75 µM (0.2% v/v DMSO) and without any cell. After 24 h incubation, 10 µL (1:10 µL) of CellQuanti-Blue reagent (at room temperature) were added in every well. The plate was slightly shaken and incubated for 4 h at 37ºC. The fluorescence was measured with a microplate spectrophotometer at a wavelength of 530 nm (excitation) and 590 nm (emission).

***Bacteria assays:***

Bacterial culture plates were prepared with 20 g of TSA dissolved in 500 mL of distilled water and autoclaved for 45 min. TSB medium was also prepared with 15 g of TSB dissolved in 500 mL of distilled water and autoclaved for 45 min. A colony of *Staphylococcus Aureus* was placed into a tube containing 4 mL of TSB and shaken (150 rpm) at 37ºC overnight.

A sample of TSB (500 µL) in presence of different concentrations of croconaine (18.75 µM, 37.5 µM and 75 µM) was irradiated for 5min (800nm, 2W/$cm^2$) and the temperature reached was monitored. The assays were performed under 37ºC atmosphere. A TSB medium blank and a water blank without croconaine were also performed.

Bacteria thermal death evaluation was performed once a stationary phase (i.e., the $10^9$ CFU/mL) was reached. The solution was dissolved until $10^5$ CFU/mL and placed in a 52ºC incubator (3x500 µL) for 5 min. A blank control was incubated in a 37ºC incubator (3x500 µL) for 5 min, 20 min and 30 min. The samples were dissolved until $10^4$, $10^3$, $10^2$ and 10 CFU/mL and seeded (25 µL per drop) on the culture plates previously prepared. After 24 h incubation (37ºC), the colonies were counted and the colony-forming units (CFU) were calculated following equation:

$$\frac{CFU}{mL} = \frac{Colonies\ number * Dilution\ factor}{Sample\ volume\ (mL)}$$

# Chapter 04

## 4. RESULTS

### 4.1. ORGANIC SYNTHESIS

Once croconaine and croconaine-macrocycle molecules were synthesized 150 mg (58% yield) and 18 mg (10% yield) were obtained, respectively. Their structures were corroborated by NMR (ANNEX II, Figures 37 and 43) and their characterizations performed. First an UV/VIS absorption analysis was carried out to check out their absorption behavior.

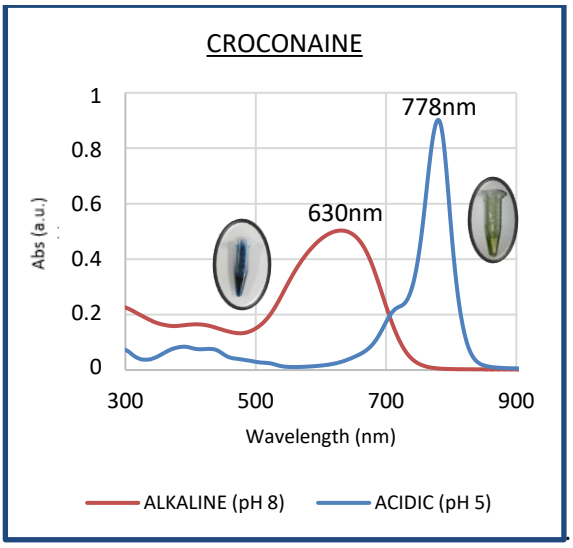


*Figure 9. UV/VIS absorption plot of acidic and alkaline croconaine in ethanol solutions (16 µM)*

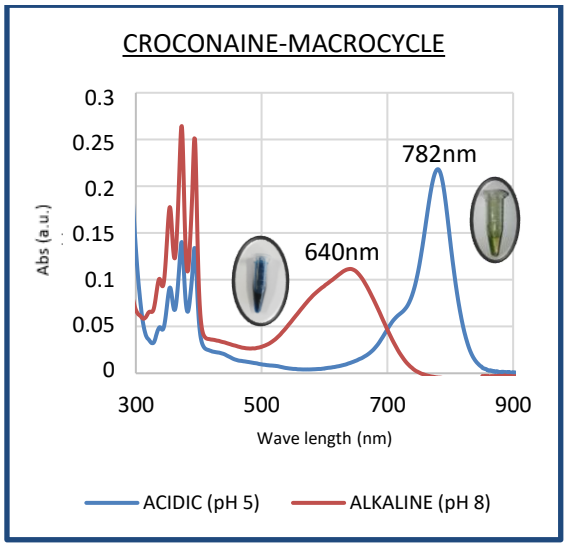


*Figure 10. UV/VIS absorption plot of acidic and alkaline croconaine-macrocycle in ethanol solutions (16 µM)*

As shown in Figure 9 and 10, both molecules have a specific high absorption peak around 800 nm in the presence of acidic pH, and a lower one around 600 nm in the presence of alkaline

pH. Moreover, the croconaine-macrocycle presents about 10 nm red-shift of both croconaine absorption maxima. On the other hand, even if the croconaine-macrocycle NMR did not show any presence of free croconaine, there was still some empty macrocycle remaining, which can also be appreciated in the UV/VIS absorption plot (Figure 10) around 400 nm.

A laser irradiation assay was carried out in order to monitor the temperature increase when croconaine is induced to its acidic structure in an ethanol-HCl solution, reaching a temperature increase of 36ºC in 15 min (ANNEX III, Figure 56).

It was also performed a reactive oxygen species (ROS) study to verify if there were ROS generation, and to corroborate the potential therapy would be exclusively based on thermal ablation. Dihydrorhodamine 123 was used as the indicator given that in the presence of ROS it suffers an oxidation turning into its cationic form (rhodamine 123), a fluorescent dye [40], therefore, a fluorescence emission reading can be carried out showing an emission maximum at 530 nm.

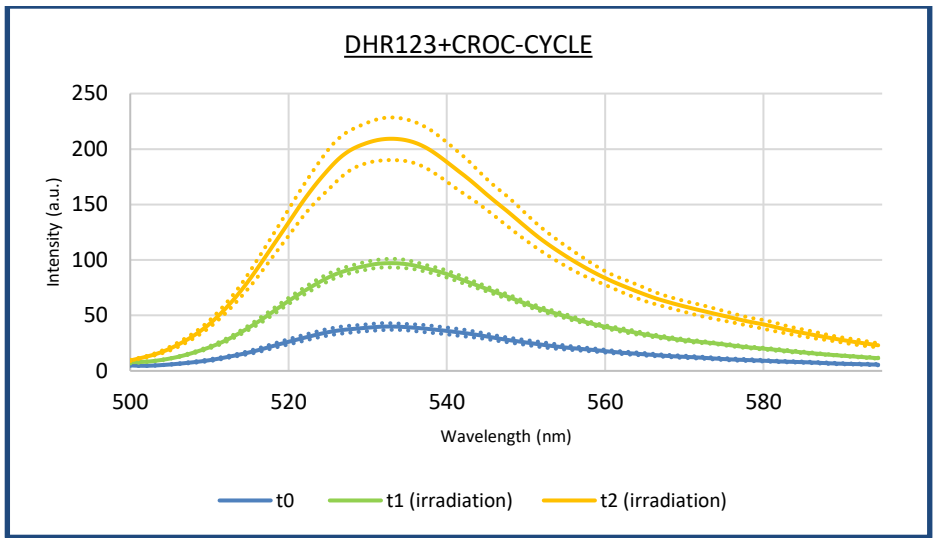


*Figure 11. Fluorescence emission plot for croconaine-macrocycle and DHR123 solution (acidic ethanol solution), after 5 min irradiation (t1) and 10 min irradiation (t2) at 808 nm and 2 W/cm².*

As shown in Figure 11, there is a relation between the irradiation time and the ROS generation. After 5 minutes irradiation, the mixture fluorescence increased about 60 units, and after 5 more minutes irradiation, the fluorescence increased 110 more units. Additionally, several controls were performed in order to assure if the ROS released were just related to the irradiation. First of all, it was measured the fluorescence emitted by the croconaine-macrocycle itself after 5 min irradiation, and the acidic ethanol solution by itself again after 5 min irradiation. In both cases, no fluorescence emission was measured (ANNEX III, Figure 45). Secondly, the fluorescence emitted by the DHR123 was tested under different scenarios: after 5 min stirring, after 5 min irradiation and after 5 min under a 46ºC water bath, which is the same temperature reached on the irradiated croconaine solution (ANNEX III, Figure 46). As observed in Figure 46, DHR123 suffers a spontaneous oxidation when heated at 46ºC (about 80 units increase), which leads to a final control to verify this DHR123 influence on the results previously obtained.

As expected, there is a ROS generation increase when only temperature (46ºC) is applied on the sample, croconaine-macrocycle with DHR123 for 5 min (20 units increase), and even some increase when only stirring it for 5 min (10 units increase). Hence, the real irradiation influence on the ROS liberation is about 30 units (Figure 12).

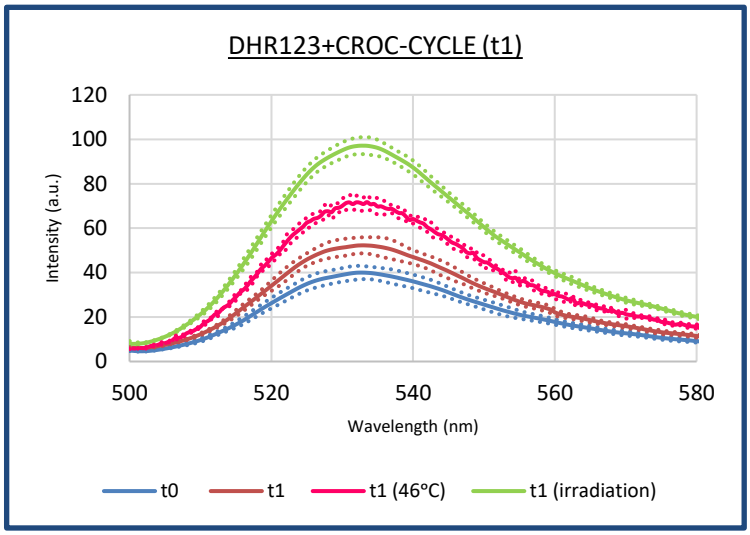


*Figure 12. Fluorescence emission plot for croconaine-macrocycle and DHR123 solution (acidic ethanol solution), after 5 min stirring (t1), 5 min stirring in a water bath at 46°C and 5min irradiation at 808 nm and 2 W/cm2.*

## 4.2. NANOPARTICLE SYNTHESIS

***Nanoprecipitation method***

Dynamic light scattering (DLS), scanning electron microscopy (SEM) and transmission electron microscopy (TEM) were used to determine the nanoparticles size when synthesized with and without the croconaine-macrocycle. Since DLS measures the hydrodynamic diameter, considering the hydration layer surrounding the particle, the NPs size obtained were larger than the ones obtained by SEM or TEM, as expected. Yet SEM measured diameters are larger than TEM's ones because of the Au-Pd covering used for observation, which provides several nanometres of Pd on the surface of each NP (Table 1 and Figure 13).

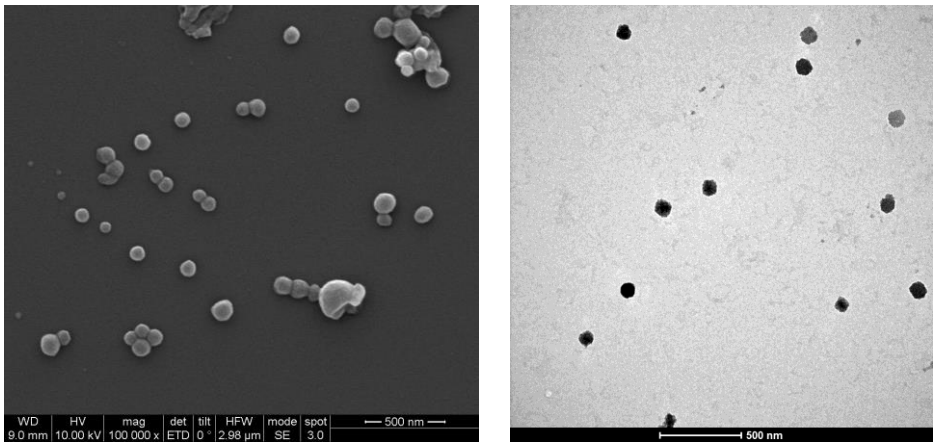


*Figure 13. On the left, SEM image of empty PLGA-PEG NPs; on the right TEM image of empty PLGA-PEG NPs.*

*Table 1. Empty PLGA-PEG NPs diameter measured by DLS, SEM and TEM*

| DLS | SEM | TEM |
|---|---|---|
| 234.9 ± 13.4nm | 97.7 ± 5.7nm | 78.2 ± 9.2nm |

Considering that SEM provided a more realistic diameter approach than DLS, offered more information, such as nanoparticles morphology, and had a better accessibility than to a TEM, it was selected as the characterization technique to proceed with the characterization and compare the different NP synthesis methods.

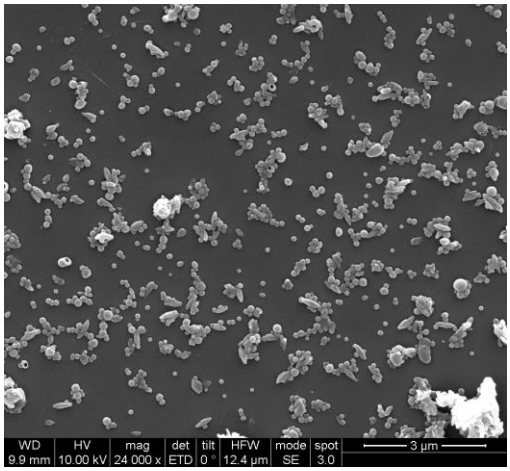


*Figure 14. SEM image of croconaine-macrocycle loaded PLGA-PEG NPs (nanoprecipitation method)*

Once croconaine-macrocycle was encapsulated, from the SEM images taken (Figure 14), it can be observed that spherical shaped NPs were obtained, some of them agglomerated, with a high monodispersity, fitted by a narrow Gaussian distribution (ANNEX III, Figure 47), and centred around an average diameter of 118.2 nm ± 6.7 nm after measuring 200 randomly selected particles from each replica. It can also be identified some polymer aggregates which could be perfectly removed passing through a 0.45 µm filter.

To check if the NPs loaded with croconaine-macrocycle respond to alkaline and acidic medium, a UV/VIS absorption analysis was performed. According to Figure 15, a slight peak appears at 813.5 nm which matches with the acidic absorbance peak. Nevertheless, when the sample was dissolved into an alkaline medium, the same absorbance plot was obtained. In order to verify that this phenomenon was not a matter of time or concentration, hypothesizing that the croconaine-macrocycle molecules were in their acidic structure initially, a new test was performed to measure the absorbance 24 h later to provide with enough time for the solvent to diffuse in the nanoparticles and thus shifting the structure of the contained croconaine. Also, the croconaine-macrocycle concentration used in the synthesis was doubled to evaluate if the polymer absorption signal hided the alkaline absorption peak (ANNEX III, Figures 51 and 52).

However, none of this hypothesis ended up being accepted given that, again, when the samples were put into alkaline medium both tests showed an identical signal as the first one measured. Hence no pH-dependence for the retrieved signal was obtained.

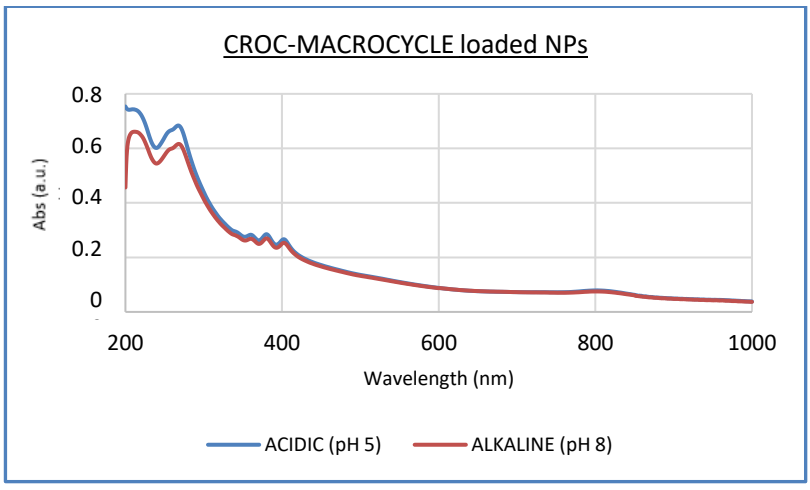


*Figure 15. UV/VIS absorption plot of croconaine-macrocycle loaded NPs in acidic and alkaline water media*

Besides, to prove that croconaine molecules (without the macrocycle) aggregates when encapsulated, a UV/VIS absorption test was performed. Analysing Figure 16, it can be noticed that no croconaine characteristic peaks appear, neither at 600 nm for the alkaline pH or at 800 nm for the acidic pH.

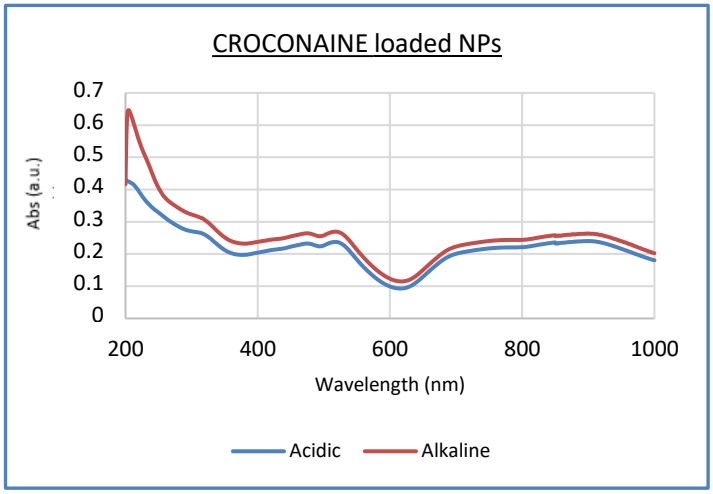


*Figure 16. UV/VIS absorption plot of croconaine loaded NPs in acidic and alkaline water media*

***Double emulsion method***

Once the double emulsion PLGA NPs were synthesized, their SEM characterization was performed showing a spherical shaped NPs with no-agglomeration (Figure 17), and little polydispersity centered at 116 nm ± 20.1 nm average diameter (croconaine-macrocycle loaded NPs) (ANNEX III, Figure 48). In this synthesis, no relevant polymer aggregates were noticed.

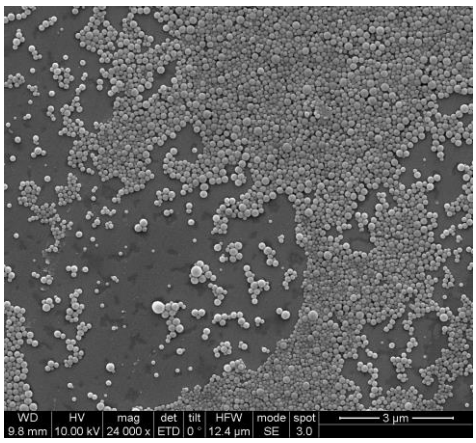


*Figure 17. SEM image of croconaine-macrocycle loaded PLGA NPs (double emulsion method)*

When samples were dispersed into the alkaline medium (PBS in water), an interesting phenomenon happened. As shown in Figure 18a, the NPs, both empty or croconaine-macrocycle loaded, dispersed into the acidic medium presented an appropriate solution stability, and even the acidic characteristic absorbance peak appeared around 787 nm (Figure 20). However, when the NPs were dispersed into the alkaline medium (PBS in water) the solution precipitated (Figure 18b) and no characterization was possible.

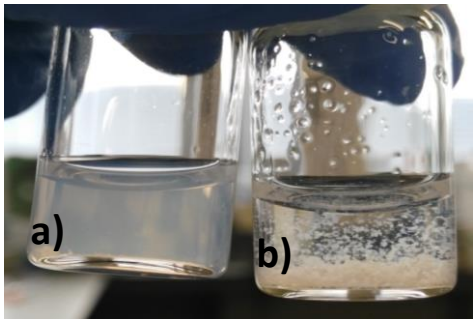


*Figure 18. a) PLGA NPs dispersed into acidic medium (HCl in water); b) PLGA NPs dispersed into alkaline medium (PBS in water)*

Therefore, another alkaline medium was prepared using NaOH instead of PBS buffer. While empty NPs sample presented a good stability in this new alkaline medium (Figure 19a), the croconaine-macrocycle loaded NPs at first sight disappeared (Figure 19b). Afterwards, the UV/VIS absorbance plot (Figure 21) showed that no polymer NPs were left in this last solution and thus the Croconaine-macrocycle was released under its alkaline structure, since a 654 nm peak appeared (ANNEX III, Figure 53). Moreover, a DLS analysis was carried out proving that no particles were left, and even a SEM characterization shows an agglomerate mass of organic material (ANNEX III, Figure 54), so no trace of nanoparticles was found.

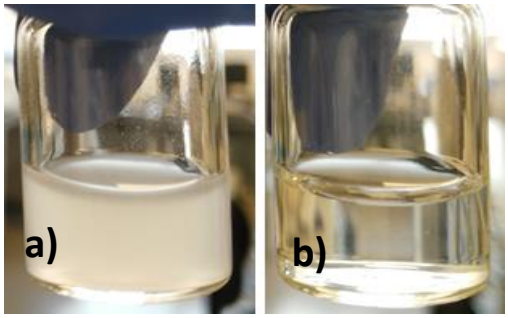


*Figure 19. a) empty PLGA NPs dispersed into alkaline medium (NaOH in water); b) croconaine-macrocycle loaded PLGA NPs dispersed into alkaline medium (NaOH in water)*

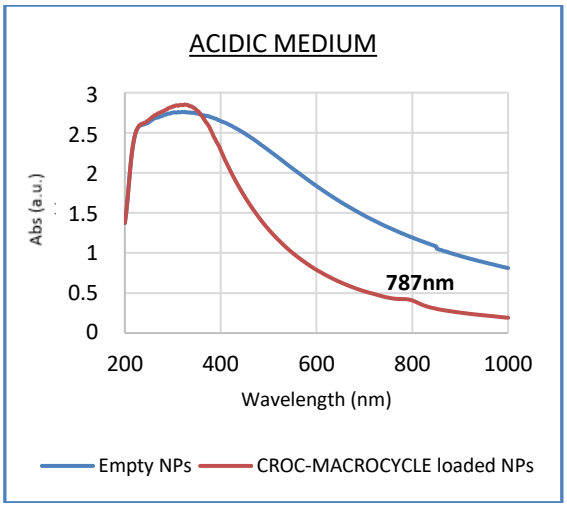


*Figure 20. UV/VIS absorption plots of croconaine-macrocycle loaded NPs, and empty NPs (double emulsion method) in acidic water medium.*

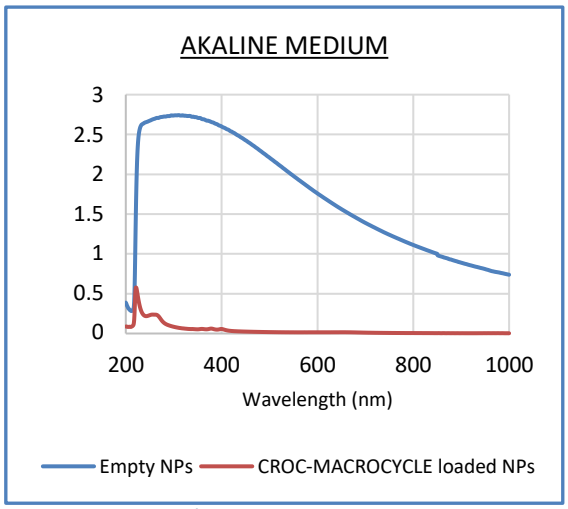


*Figure 21. UV/VIS absorption plots of croconaine-macrocycle loaded NPs, and empty NPs (double emulsion method) in alkaline water medium.*

At that point, an alternative double emulsion synthesis was carried out, using cationic surfactants instead of sodium cholate, since previously reported by S. Guha et al. [16], croconaine was inserted in their liposomal membrane forming an amphiphilic ion-pair with a cationic surfactant. The first one used was poly(allylamine hydrochloride) (PAH), a polyelectrolyte, although when re-suspended into the water the polymer precipitated meaning no nanoparticles were formed.

The second one was hexadecyltrimethylammonium bromide (CTAB) an amphiphilic cationic surfactant.

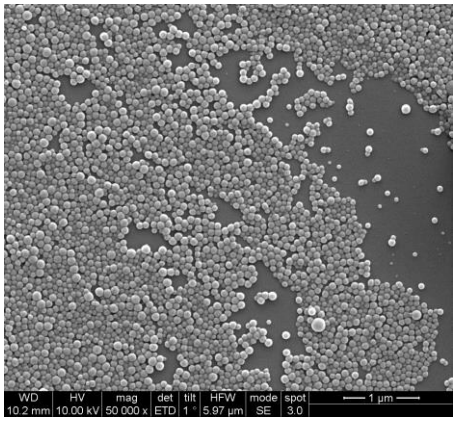


*Figure 22. SEM image of croconaine-macrocycle loaded PLGA NPs (double emulsion method with CTAB as surfactant)*

In this case a homogeneous tapestry of spherical shaped nanoparticles was formed, as showed in Figure 22, with no polymer aggregates, and little polydispersity (ANNEX III, Figure 49). Also, a smaller size of nanoparticles was achieved having an average diameter of 75 nm ± 11.2 nm both empty and loaded NPs. Moreover, when the samples were dispersed into acidic and alkaline mediums the solutions remained stable. However, the UV/VIS absorbance plots showed that, again, the characteristic peak observed under acidic condition could be discerned, but not the alkaline one (Figure 23).

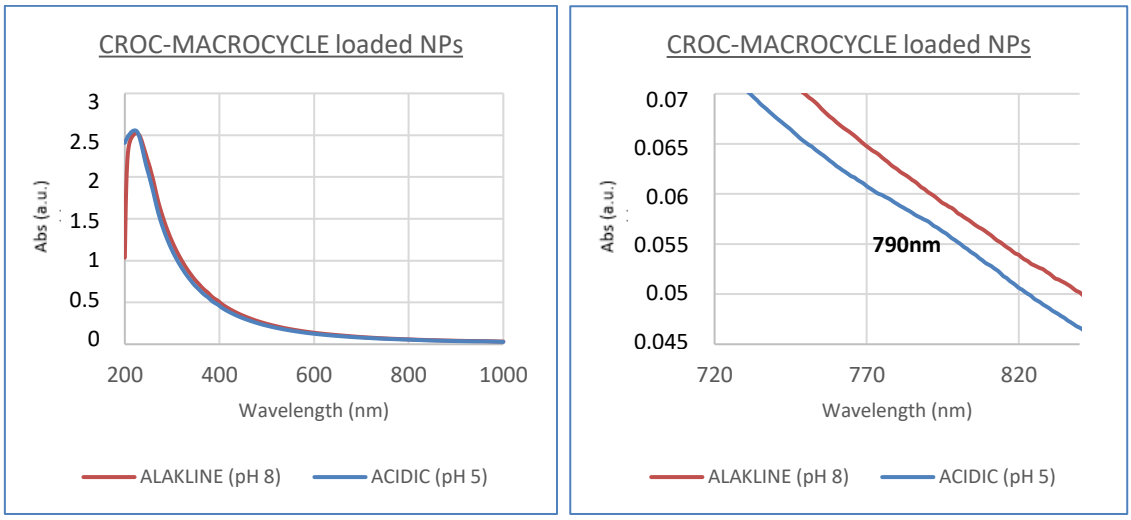


*Figure 23. UV/VIS absorption plots of croconaine-macrocycle loaded PLGA NPs (double emulsion method with CTAB) in acidic and alkaline water media.*

A double croconaine-macrocycle concentration synthesis was also performed but, yet no absorbance peak appeared around 600 nm in the alkaline medium (ANNEX III, Figure 55).

A laser irradiation assay was carried out, monitoring the temperature increase of the acidic samples, to check its efficiency as a photothermal nanoparticulated agent (ANNEX III, Figure 57). But only a 3ºC increase was achieved after 15 min versus the 36ºC increase achieved by the free croconaine-macrocycle under the same laser exposure time and irradiance (ANNEX III, Figure 56).

Finally, a last cationic surfactant was tested, the cholesteryl 3β-N-(dimethylaminoethyl)-carbamate hydrochloride (DC-Cholesterol) a cationic cholesterol derivate.

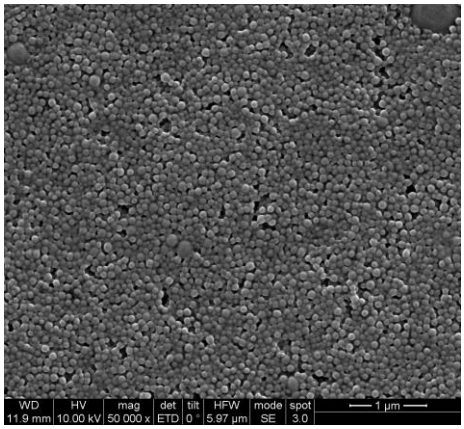

*Figure 24. SEM image of croconaine-macrocycle loaded PLGA NPs (double emulsion method with DC-Cholesterol as surfactant)*

In this occasion the SEM images (Figure 24) revealed the formation of the nanoparticles, again spherical shaped with reduced polydispersity, fitted by a Gaussian curve (ANNEX III, Figure 50), although a light agglomeration between the particles was observed. An average diameter of 74.4 nm ± 13.1 nm was obtained, and some polymer aggregates were found (Figure 24). Once more, the samples remained stable when solved into acidic and alkaline media, and no alkaline peaks were noticed at the UV/VIS absorption plot (Figure 25). Neither a relevant temperature increase was monitored when the acidic sample was irradiated (ANNEX III, Figure 58).

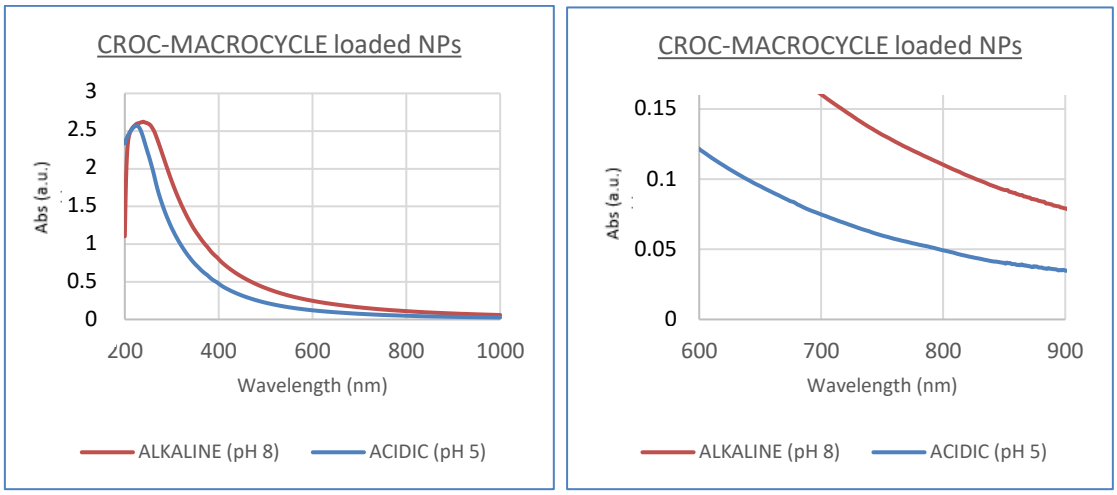


*Figure 25. UV/VIS absorption plots of croconaine-macrocycle loaded PLGA NPs (double emulsion method with CTAB) in acidic and alkaline water media.*

Table 2 shows a summary of all the particles sizes of the polymeric encapsulations carried out in this study.

*Table 2. Polymeric nanoparticles diameter summary*

| | **Nanoprecipitation** | **Double Emulsion (Sodium Cholate)** | **Double Emulsion (CTAB)** | **Double Emulsion (Dc-Cholesterol)** |
|---|---|---|---|---|
| **Empty NPs** | 97.7nm ± 5.7nm | 98.2nm ± 18.2nm | 75.3nm ± 12.8nm | - |
| **Croconaine-macrocycle loaded NPs** | 118.2nm ± 6.7nm | 116nm ± 20.1nm | 75nm ± 11.2nm | 74.4nm ± 13.1nm |

***Niosomes***

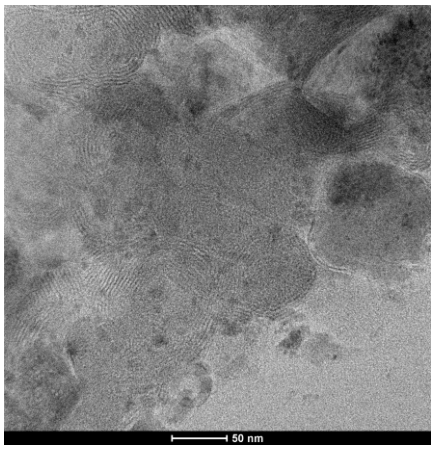


*Figure 26. TEM image of croconaine-macrocycle loaded niosomes*

For the niosomes characterization TEM, instead of SEM, was used since this last one did not allow their multilayer visualization with enough resolution. As shown in Figure 26, assorted multilayer niosomes were obtained, composed from 2 to more than 8 layers.

However, due to the high amount of croconaine-macrocycle needed for this synthesis, it was only possible to produce it once. Thus, the average diameter is based on just one replica, obtaining 78nm.

UV/VIS absorbance assays were performed, and once again, no alkaline peak could be distinguished, it even appeared at the same wavelength of the acidic peak (Figure 27).

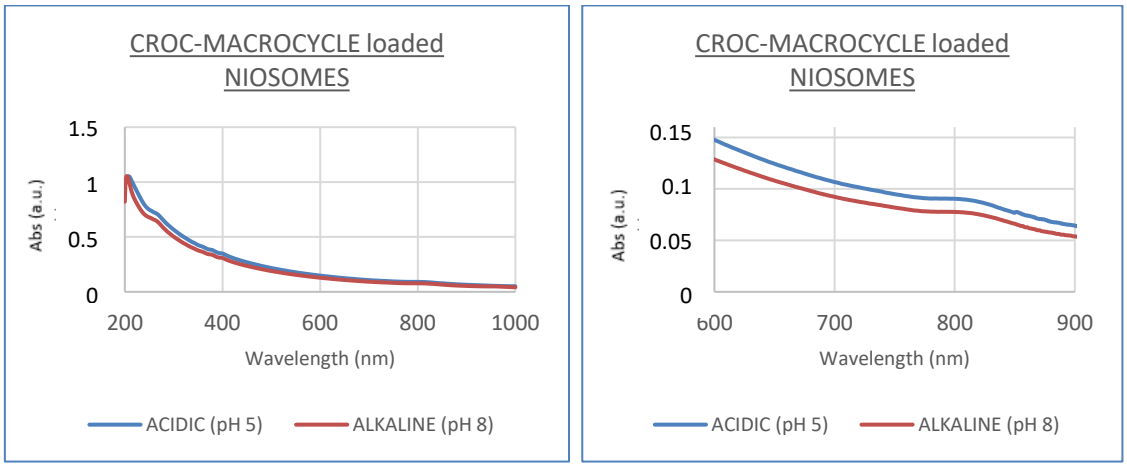


*Figure 27. UV/VIS absorption plot of croconaine-macrocycle loaded niosomes in acidic and alkaline water media.*

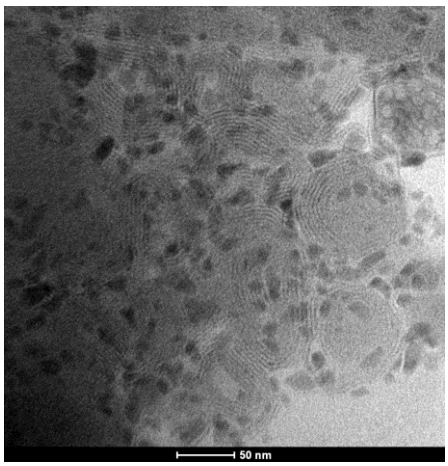


*Figure 28. TEM image of croconaine-macrocycle loaded niosomes (using CTAB surfactant)*

A new synthesis was attempted using CTAB cationic surfactant instead of dihexadecyl phosphate (DCP) as component of the niosomal membrane, to verify if again there was an interaction between this component and the croconaine.

The niosomes obtained had again a varied number of layers and an average diameter around 94nm (Figure 28).

When they were tested through UV/VIS absorbance technique, a similar plot was obtained (Figure 29) as the one earlier shown (Figure 27).

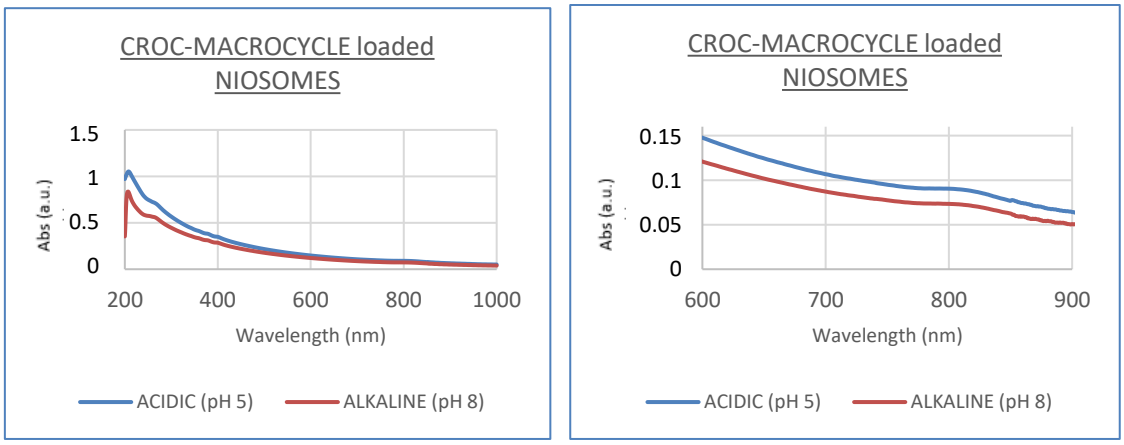


*Figure 29. UV/VIS absorption plot of croconaine-macrocycle loaded niosomes (using CTAB surfactant) in acidic and alkaline water media.*

Nevertheless, when the acidic sample was irradiated, a reduced 5.6°C increase was achieved after 15 min, almost the same than the one obtained when the alkaline sample was irradiated (6.3°C) (ANNEX III, Figure 60).

## 4.3. BIOLOGICAL STUDIES

***Cytotoxicity assay***

The cell cytotoxicity was studied *in vitro* using THP-1 cells, after 24h of incubation with croconaine, and following the Blue Cell Viability Assay Kit. As shown in Figure 30, cell viability remained higher than 90% at any croconaine concentration tested, even at 75 µM which showed a 93.8% ± 2.9% cell viability.

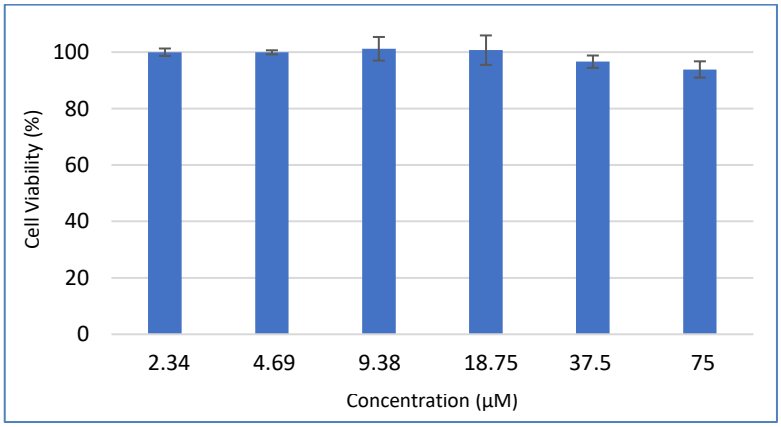


*Figure 30. Croconaine cytotoxicity determined by Blue Cell Viability Assay Kit (Abnova Protocol) for different concentrations of the molecule.*

Since no encapsulation really worked for a potential PTT, because no pH dependent response was observed, it wasn't possible to continue with the *in vitro* assays.

***Bacteria assays***

To proceed with the cell infection model assay, initially, the maximum temperature achieved by the croconaine when irradiated in cell medium (RMPI 1640) was evaluated.

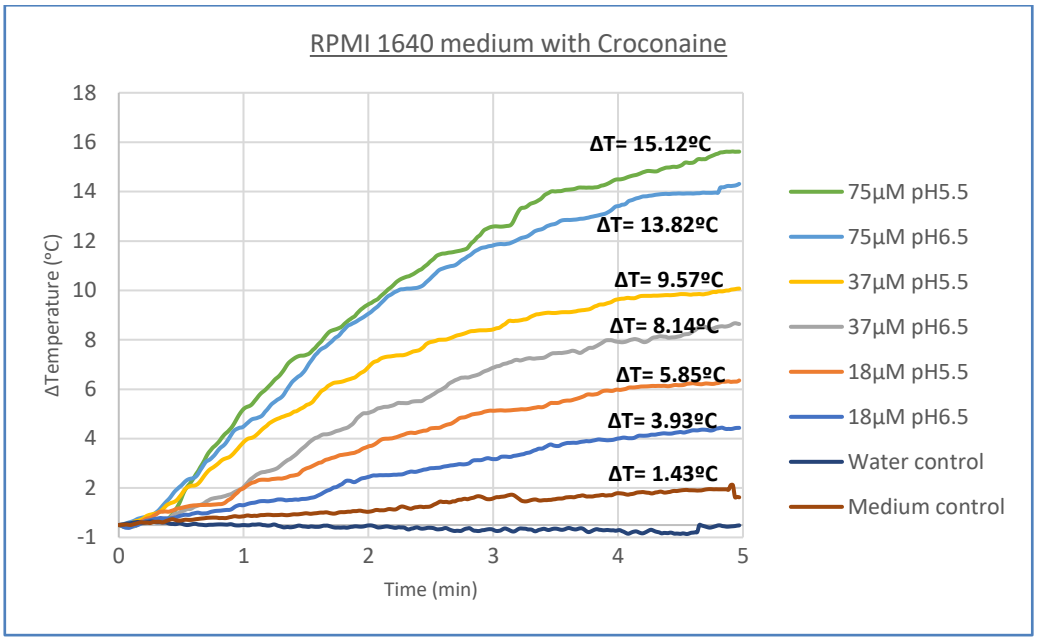


*Figure 31. Temperature change curves of croconaine in RPMI 1640 medium solution (75, 37 and 18 µM) at different pH values (5.5 and 6.5) with laser irradiation (808 nm, 2 W/cm², 5 min).*

As shown in Figure 31, when the highest concentration sample (75 µM) was irradiated for 5 min, a 15°C increase was reached, in an acidic medium of pH 5.5.

Considering this, a new test was performed in order to verify if the pathogenic *S. Aureus* would be eliminated in a quick thermal ablation. Once the colonies ($10^5$ CFU/mL) were incubated at 52°C for 5 min, no relevant death was noticed. The incubation time was increased at 20 min, but again, no relevant death was noticed. Finally, a last test was performed heating a reduced colony loading of $10^2$ CFU/mL for 20 min, and once again, no relevant death was noticed (Table 3).

*Table 3. S. Aureus colony-forming unit after a thermal ablation at 52°C incubation, for 5 min and 20 min, starting from a $10^5$ CFU/mL colony counts and (*) a $10^2$ CFU/mL colony counts. The counting process was realized after 24h incubation of the treated colonies*

| | **Control at 37°C** | **Sample at 52°C** |
|---|---|---|
| **5 min Incubation** | $1.5 \cdot 10^6 \pm 1.2 \cdot 10^5$ CFU/mL | $1.1 \cdot 10^6 \pm 1.7 \cdot 10^5$ CFU/mL |
| **20 min Incubation** | $2.8 \cdot 10^6 \pm 3.4 \cdot 10^5$ CFU/mL | $1.1 \cdot 10^6 \pm 9.9 \cdot 10^4$ CFU/mL |
| **20 min Incubation*** | $7.6 \cdot 10^5 \pm 2.3 \cdot 10^5$ CFU/mL | $3.1 \cdot 10^5 \pm 4.7 \cdot 10^4$ CFU/mL |

Since none of the assays proved a positive result, it wasn't possible to continue with the cell infection model.

# Chapter 05

## 5. DISCUSSION

### 5.1. ORGANIC SYNTHESIS

In this work, an almost pure croconaine-macrocycle compound was obtained, although some empty macrocycle was remaining. This fact was already described by S. Guha et al. [16], who reported a similar UV/VIS absorption spectrum (Figure 5b) as the one obtained in this study. The presence of this empty macrocycle does not interfere with the following experiments due to its negligible absorbance at 800nm. However, that is a fact to keep in mind since the measured concentration of the compound will not be considered fully pure croconaine-macrocycle.

Besides, S. Guha et al. [16] stated a 20 nm red-shift among the free croconaine and the croconaine-macrocycle absorption peaks, which differs from the 10 nm obtained herein. This outcome could be on account of the solvent used as medium, as a change in the dielectric constant of the surrounding medium can shift the absorption maximum. For their experiment, S. Guha et al. used chloroform as a solvent instead of ethanol as we did.

In addition, when croconaine-macrocycle was irradiated with the laser (808 nm, 2 W/cm$^2$) a 36ºC temperature increase was achieved using only 16 µM which is three times more than the temperature increase achieved by ICG or IR780 under the same conditions [16].

***ROS formation***

As reported by some research groups, croconaine dye produces a reduced singlet oxygen generation [16][17]. In the present study it has been demonstrated that there was a presence of ROS when the sample containing croconaine-macrocycle was irradiated, although, to be able to quantify it, it would be required a more specific test involving, for instance, cellular cultures, (CellROX® provides several kits for the detection and quantitation of reactive oxygen species (ROS) in cells).

## 5.2. NANOPARTICLE SYNTHESIS

***Nanoprecipitation method***

Regarding to the simple croconaine encapsulation and its UV/VIS absorbance characterization, it has been demonstrated that croconaine self-aggregates within the encapsulating nanoparticle causing an absorbance quenching and thus losing the characteristic croconaine absorbance peaks, for neither the alkaline or the acidic configuration, just as S. Guha et al. reported [16].

On the other hand, in this work, a final hypothesis concerning the results attained when croconaine-macrocycle was encapsulated by nanoprecipitation method has been proposed. Assuming that the croconaine-macrocycle was encapsulated under its acidic structure, the possible PLGA-PEG natural degradation could have acidified the inner medium of the nanoparticles keeping the molecule at the same acidic structure even if the outer medium was alkaline. This would also be justified considering that this method stores the molecules inside the nanoparticle instead of having them along the polymeric structure and in direct contact with the medium. So, the acidic degradation byproducts of the encapsulating agent (lactic and glycolic acids) could reduce the pH and quench the pH-responsiveness of croconaine.

***Double emulsion method***

Considering that PLGA is a pH sensible polymer with different degradation rates depending on the pH, specially faster at alkaline pH [21], and the absence of PEG on this formulation, it has been set out the idea of a destabilization of the nanoparticle and the consequent polymer precipitation due to the PBS presence, whereas under the presence of NaOH, the polymer dissolved. Moreover, it can also be justified by resuming the hypothesis of an initial acid structure of the croconaine-macrocycle molecule, which, in this kind of structure, is disposed in the outer part of the NPs, in direct contact with the medium. When the molecule changes into an alkaline structure, the proton release could destabilize the anionic surfactant (sodium cholate), that keeps the nanoparticle together, and causes its breakout and consequent croconaine-macrocycle release.

Nevertheless, when the cationic surfactants were used, in the presence of alkaline medium the nanoparticles remained stable as the released proton did not interact with them. This fact can be supported by S. Guha et al. whom used a cationic surfactant to create an amphiphilic ion-pair in their liposomes [16]. The first cationic surfactant tested, PAH, was not able to even create the nanoparticles with this synthesis protocol due to its huge chain length ($M_W$ ~15000 Da). The second one, CTAB, is a popular cationic surfactant widely used [6][44]. It allowed the formation of spherical nanoparticles with good stability at different pH variations, although, unbound CTAB is an already reported cytotoxic surfactant [44]. Finally, the last cationic surfactant, DC-Cholesterol, showed a similar performance as the CTAB, but no toxicity has yet been reported. Moreover, it has a very similar structure than the cationic surfactant used by S. Guha et al., the 1,2-dioleoyl-3-trimethylammoniumpropane (DOTAP). Regarding the lack of the alkaline absorbance peak, it has been hypothesized that the polymer absorbance is too strong, and it could be overlapping with the croconaine-macrocycle one.

Even if both CTAB and DC-Cholesterol presented a good behavior as surfactants and spherical nanoparticle were formed, in any case the molecule produced the photothermal effect as

expected when irradiated with the laser. This phenomenon could be related to a low Croconaine-macrocycle encapsulation, not just because of the synthesis but also because of the presence of the empty macrocycle. And finally, concerning the absence of the alkaline peak at the UV/VIS absorbance plots can be related to the strong polymer signal, which overlaps.

***Niosomes***

The niosomes were synthesized successfully, having a multilayer structure. But once again, when niosomes were loaded with the croconaine no alkaline peak could be observed by UV/VIS absorption spectrophotometry. A first hypothesis was set out, proposing that again the anionic surfactant was the problem. However, since the new formulation with CTAB showed the same results, a final hypothesis has been suggested. The little amount of croconaine-macrocycle that has actually been encapsulated could have been trapped within the multilayers, away from the surface and thus, from the alkaline medium. This hypothesis would drove us to a new unilamellar niosome synthesis were the molecules would be more exposed to the medium.

It has also been seen that a temperature increase is notice when the both acidic and alkaline samples were irradiated, meaning that no alkaline structure was achieved but also that the croconaine inside the niosome remained functional. Although a reduced amount of it was encapsulated to reach the same temperature increase than the one obtained with free croconaine.

## 5.3. BIOLOGICAL STUDIES

On account of the little amount of croconaine-macrocycle synthesized, it was decided to proceed with the biological assays using croconaine without the macrocycle in order to set out the experimental parameters.

As seen no cytotoxicity can be attributed to the molecule since none of the concentrations tested, showed a cell viability lower than 90% [17]. Compared to the existing cytotoxicity tests concerning croconaine, already reported by S.Guha et al. [16] or L. Tang et al. [15], herein it has been proved that even at higher concentrations, the molecule is not cytotoxic (75 µM).

Therefore, the following test with bacteria were carried out using the highest concentrations previously tested, 18.75 µM, 37.5 µM and 75 µM. As proved, when the highest concentration sample (75 µM) was irradiated for 5 min, a 15ºC increase was monitored meaning that 52ºC can be reached in a biological application where the initial temperature is 37ºC and the pH is about 5.5.

Hence, the next assay was focused on eradicating *S. Aureus* by thermal ablation at 52ºC. However, when the $10^5$ CFU/mL colonies were incubated at that temperature for 5 and 20 min, no death was achieved comparing it to the control incubation at 37ºC. Then a new test was performed assuming that the colony-forming units in a wound would be much less than $10^5$ CFU/mL, but again, no positive results were obtained. Actually, other research groups have proved that it would take more than 530 min to fully kill a *S. Aureus* infection with a 54.4ºC incubation [35], and indeed, no thermal death would be possible using croconaine as a PTT agent for such a brief period of time.

# Chapter 06

## 6. CONCLUSIONS

In summary, it has been synthesized and characterized the desired molecule, the croconaine, capable of heating up a medium in a pH-dependent manner, when irradiated with a laser in the NIR region, reaching a 36ºC temperature increase with a concentration as little as 16 µM. That molecule would be internalized within the acidic endocytic vesicles of tumoral cells and only in the interior it would be activated and would efficiently absorb the light and the consequent heat. The presence of the molecule in the extracellular media would not have any cytotoxic effect.

However, none of the polymeric encapsulations tested in this study have shown the pH-dependent behavior desired, since the medium was not heated up when irradiated. Concerning the PLGA-PEG nanoparticles, the alkaline medium was not able to diffuse within the nanoparticle and trigger the change in the molecule structure; it actually showed an acidic structure all along. On the other hand, the alkaline peak characteristic of the PLGA nanoparticles was not visible either, probably due to the polymer high absorbance, which does not mean that the molecule was not on its alkaline structure. And the almost imperceptible heat increases when irradiated could be attributed to a low croconaine-macrocycle encapsulation. Finally, the only croconaine encapsulation that has presented some good outcomes, is the one carried out within niosomes, although a very small temperature increase was achieved ($\Delta T$=5.6ºC) and the alkaline structure of the molecule did not present its characteristic absorbance peak.

And finally, it has been proved that a concentration of croconaine of 75 µM remains non-cytotoxic, heating up a culture medium until 52ºC within 5 min of irradiation exposure, and making of this compound a good absorptive agent for cancer phototherapy or antimicrobial phototherapy. Even though this temperature was not enough to eradicate *S. Aureus* within a short period of irradiation at the doses tested.

***Future Steps***

The future steps for this study would include the quantification of the real croconaine-macrocycle concentration within the nanoparticles in order to meet the real encapsulation ratio and improve it. This would be useful to prove if the double emulsion nanoparticles are actually working with this duality or not.

It could also be appropriate to synthesize unilamellar niosomes and check if this was the issue that prevented the alkaline medium to change the molecular structure.

Moreover, it would be interesting to test the cytotoxicity of the croconaine-macrocycle molecule even if the free croconaine has shown positive results, as well as a quantification of the ROS generation to truly prove that it is an exclusive photothermal agent.

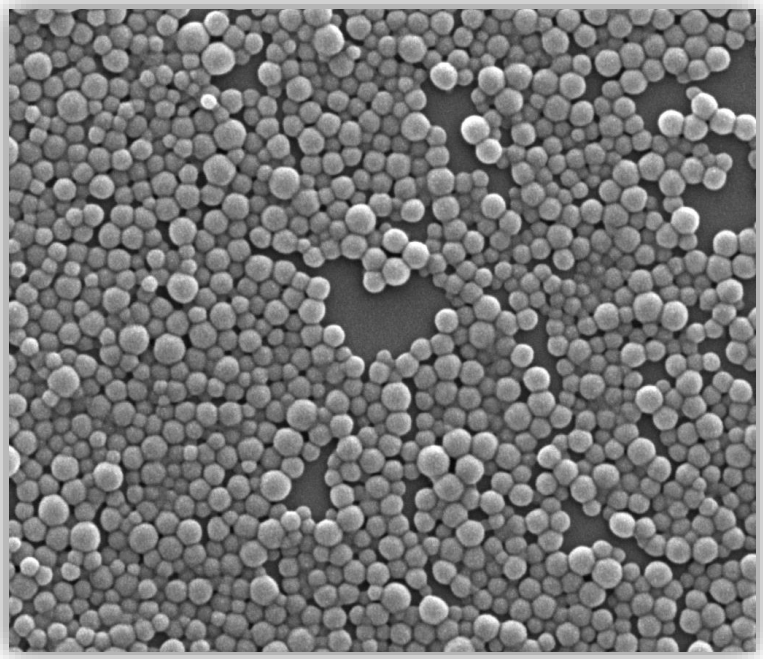

# 7. REFERENCES


[1] N. Taniguchi, "On the Basic Concept of 'Nano-Technology,'" *Japan Soc. Precis. Eng.*, vol. Part II, 1974.

[2] A. K. Singh, "The Past, Present, and the Future of Nanotechnology," *Eng. Nanoparticles*, pp. 515–525, 2016.

[3] C. Kinnear, T. L. Moore, L. Rodriguez-Lorenzo, B. Rothen-Rutishauser, and A. Petri-Fink, "Form Follows Function: Nanoparticle Shape and Its Implications for Nanomedicine," *Chem. Rev.*, vol. 117, no. 17, pp. 11476–11521, 2017.

[4] J. Shi, P. W. Kantoff, R. Wooster, and O. C. Farokhzad, "Cancer nanomedicine: progress, challenges and opportunities," *Nat. Rev. Cancer*, vol. 17, no. 1, pp. 20–37, 2016.

[5] R. A. Yokel and R. C. Macphail, "Engineered nanomaterials : exposures , hazards , and risk prevention," *J. Occup. Med. Toxicol.*, p. 6:7, 2011.

[6] Y. Huang, K. Sefah, S. Bamrungsap, H. Chang, and W. Tan, "Selective Photothermal Therapy for Mixed Cancer Cells Using Aptamer-Conjugated Nanorods Selective Photothermal Therapy for Mixed Cancer Cells Using Aptamer-Conjugated Nanorods," no. 5, pp. 11860–11865, 2008.

[7] Y. Nakamura, A. Mochida, P. L. Choyke, and H. Kobayashi, "Nanodrug Delivery: Is the Enhanced Permeability and Retention Effect Sufficient for Curing Cancer?," *Bioconjug. Chem.*, vol. 27, no. 10, pp. 2225–2238, 2016.

[8] S. Azzi, J. K. Hebda, and J. Gavard, "Vascular Permeability and Drug Delivery in Cancers," *Front. Oncol.*, vol. 3, no. August, pp. 1–14, 2013.

[9] Y. Al-Kofahi, C. Sevinsky, A. Santamaria-Pang, F. Ginty, A. Sood, and Q. Li, "Multi-channel algorithm for segmentation of tumor blood vessels using multiplexed image data," *Proc. - Int. Symp. Biomed. Imaging*, vol. 2016–June, pp. 213–216, 2016.

[10] H. Kobayashi and M. W. Brechbiel, "Nano-sized MRI contrast agents with dendrimer cores," *Adv. Drug Deliv. Rev.*, vol. 57, no. 15, pp. 2271–2286, 2005.

[11] V. Shanmugam, S. Selvakumar, and C.-S. Yeh, "Near-infrared light-responsive nanomaterials in cancer therapeutics," *Chem. Soc. Rev.*, vol. 43, no. 17, pp. 6254–6287, 2014.

[12] Q. Ban, T. Bai, X. Duan, and J. Kong, "Noninvasive photothermal cancer therapy nanoplatforms via integrating nanomaterials and functional polymers," *Biomater. Sci.*, vol. 5, pp. 190–210, 2017.

[13] S. Huang, R. K. Kannadorai, Y. Chen, Q. Liu, and M. Wang, "A narrow-bandgap benzobisthiadiazole derivative with high near-infrared photothermal conversion efficiency and robust photostability for cancer therapy," *Chem. Commun.*, vol. 51, no. 20, pp. 4223–4226, 2015.

[14] C. L. Peng, Y. H. Shih, P. C. Lee, T. M. H. Hsieh, T. Y. Luo, and M. J. Shieh, "Multimodal image-guided photothermal therapy mediated by 188Re-labeled micelles containing a cyanine-type photosensitizer," *ACS Nano*, vol. 5, no. 7, pp. 5594–5607, 2011.

[15] L. Tang *et al.*, "Croconaine nanoparticles with enhanced tumor accumulation for multimodality cancer theranostics," *Biomaterials*, vol. 129, pp. 28–36, 2017.

[16] S. Guha, G. K. Shaw, T. M. Mitcham, R. R. Bouchard, and B. D. Smith, "Croconaine rotaxane for acid activated photothermal heating and ratiometric photoacoustic imaging of acidic pH," *Chem. Commun.*, vol. 52, no. 1, pp. 120–123, 2016.

[17] K. M. Harmatys, P. M. Battles, E. M. Peck, G. T. Spence, F. M. Roland, and B. D. Smith, "Selective photothermal inactivation of cells labeled with near-infrared croconaine dye," *Chem. Commun.*, vol. 53, no. 71, pp. 9906–9909, 2017.

[18] J. R. Casey, S. Grinstein, and J. Orlowski, "Sensors and regulators of intracellular pH," *Nat. Rev. Mol. Cell Biol.*, vol. 11, no. 1, pp. 50–61, 2010.

[19] S. Wang *et al.*, “Photothermal effects of supramolecularly assembled gold nanoparticles for the targeted treatment of cancer cells,” *Angew. Chemie - Int. Ed.*, vol. 49, no. 22, pp. 3777–3781, 2010.

[20] J. Chan, P. Valencia, L. Zhang, R. Langer, and O. Farokhzad, “Polymeric nanoparticles for drug delivery.,” *Methods Mol. Biol. (Clifton, N.J.) [Methods Mol Biol]*, vol. 624, pp. 163–75, 2010.

[21] H. Makadia and S. Siegel, “Poly Lactic-co-Glycolic Acid (PLGA) as Biodegradable Controlled Drug Delivery Carrier,” *J. Polym. Sci. Part B Polym. Phys.*, vol. 3, no. 49, pp. 1377–1397, 2011.

[22] S. Davaran, M. R. Rashidi, B. Pourabbas, M. Dadashzadeh, and N. M. Haghshenas, “Adriamycin release from poly(lactide-co-glycolide)-polyethylene glycol nanoparticles: Synthesis, and in vitro characterization,” *Int. J. Nanomedicine*, vol. 1, no. 4, pp. 535–539, 2006.

[23] E. Locatelli and M. C. Franchini, “Biodegradable PLGA-b-PEG polymeric nanoparticles: Synthesis, properties, and nanomedical applications as drug delivery system,” *J. Nanoparticle Res.*, vol. 14, no. 12, pp. 1–17, 2012.

[24] D. E. Owens and N. A. Peppas, “Opsonization, biodistribution, and pharmacokinetics of polymeric nanoparticles,” vol. 307, pp. 93–102, 2006.

[25] S. Hosseininasab *et al.*, “Synthesis, Characterization, and *In vitro* Studies of PLGA-PEG Nanoparticles for Oral Insulin Delivery,” *Chem. Biol. Drug Des.*, vol. 84, no. 3, pp. 307–315, 2014.

[26] E. Luque-Michel, V. Sebastian, B. Szczupak, E. Imbuluzqueta, J. Llop, and M. J. Blanco Prieto, “Visualization of hybrid gold-loaded polymeric nanoparticles in cells using scanning electron microscopy,” *J. Drug Deliv. Sci. Technol.*, vol. 42, pp. 315–320, 2017.

[27] K. B. Makeshwar and S. R. Wasankar, “Niosome : a Novel Drug Delivery System,” vol. 3, no. 1, pp. 16–20, 2013.

[28] A. Nasir, H. Sl, and K. Amanpreet, “NIOSOMES : AN EXCELLENT TOOL FOR DRUG DELIVERY,” vol. 2, no. 2, pp. 479–487, 2012.

[29] D. Paolino, D. Cosco, R. Muzzalupo, E. Trapasso, N. Picci, and M. Fresta, “Innovative bola-surfactant niosomes as topical delivery systems of 5-fluorouracil for the treatment of skin cancer,” *Int. J. Pharm.*, vol. 353, no. 1–2, pp. 233–242, 2008.

[30] S. Tamizharasi, A. Dubey, V. Rathi, and R. Jc, “Development and Characterization of Niosomal Drug Delivery of Gliclazide,” pp. 205–209.

[31] S. Moghassemi and A. Hadjizadeh, “Nano-niosomes as nanoscale drug delivery systems : An illustrated review,” *J. Control. Release*, vol. 185, pp. 22–36, 2014.

[32] A. J. Makowski, “In Vivo Analysis of Laser Preconditioning in Incisional Wound Healing of Wild-Type and HSP70 Knockout Mice With Raman Spectroscopy,” vol. 244, no. December 2011, pp. 233–244, 2012.

[33] M. S. Khan, M. L. Bhaisare, J. Gopal, and H. Wu, “Journal of Industrial and Engineering Chemistry Highly efficient gold nanorods assisted laser phototherapy for rapid treatment on mice wound infected by pathogenic bacteria §,” vol. 36, pp. 49–58, 2016.

[34] L. M. Bush, “Infecciones por Staphylococcus aureus,” *Manual MSD*. [Online]. Available: http://www.msdmanuals.com/es-es/hogar/infecciones/infecciones-bacterianas/infecciones-por-staphylococcus-aureus.

[35] N. Resources, K. Branch, R. Branch, V. Faculty, and T. Branch, “Thermal Death Time of Staphylococcus Aureus ( PTCC = 29213 ) and Staphylococcus Epidermidis ( PTCC = 1435 ) in Distilled Water,” vol. 5, no. 11, pp. 1551–1554, 2011.

[36] A. Bugarin and B. T. Connell, “Chiral Nickel ( II ) and Palladium ( II ) NCN-Pincer Complexes Based on Substituted Benzene : Synthesis , Structure , and Lewis Acidity,” no. Ii, pp. 4357–4369, 2008.

[37] B. Altava, M. I. Burguete, B. Escuder, S. V Luis, and M. C. Mufioz, “Pertosylated

Polyaza[n](9,10)anthracenophanes," vol. 53, no. 7, pp. 2629–2640, 1997.
[38] J. J. Gassensmith *et al.*, "Self-assembly of fluorescent inclusion complexes in competitive media including the interior of living cells," *J. Am. Chem. Soc.*, vol. 129, no. 48, pp. 15054–15059, 2007.
[39] J. Cheng *et al.*, "Formulation of functionalized PLGA-PEG nanoparticles for in vivo targeted drug delivery," *Biomaterials*, vol. 28, no. 5, pp. 869–876, 2007.
[40] B. Brawek *et al.*, "Reactive oxygen species (ROS) in the human neocortex: Role of aging and cognition," *Brain Res. Bull.*, vol. 81, no. 4–5, pp. 484–490, 2010.
[41] I. Ortiz De Solorzano *et al.*, "Microfluidic Synthesis and Biological Evaluation of Photothermal Biodegradable Copper Sulfide Nanoparticles," *ACS Appl. Mater. Interfaces*, vol. 8, no. 33, pp. 21545–21554, 2016.
[42] M. Prieto *et al.*, "Light-Emitting Photon-Upconversion Nanoparticles in the Generation of Transdermal Reactive-Oxygen Species," *ACS Appl. Mater. Interfaces*, p. acsami.7b14812, 2017.
[43] Abnova, "Cell Viability Assay Kit," *J. Immunol. Methods*, vol. 1, pp. 2–4.
[44] E. E. Connor, J. Mwamuka, A. Gole, C. J. Murphy, and M. D. Wyatt, "Gold nanoparticles are taken up by human cells but do not cause acute cytotoxicity," *Small*, vol. 1, no. 3, pp. 325–327, 2005.